https://doi.org/10.18321/ectj1326

Key Peculiarities of the Pyrolysis Behavior of Different Rank Coals, and Characterization of the Pyrolysis Products

P.N. Kuznetsov[1,2]*, O.Y. Fetisova[2], L.I. Kuznetsova[2], X. Fan[3], B. Avid[4], B. Purevsuren[4]

[1]Siberian Federal University, Institute of Petroleum and Gas, pr. Svobodny, 82, Krasnoyarsk, Russia
[2]Institute of Chemistry and Chemical Technology SB RAS, Federal Research Center "Krasnoyarsk Science Center SB RAS", str. Akademgorodok 50/24, Krasnoyarsk, Russia
[3]College of Chemical and Biological Engineering, Shandong University of Science and Technology, 579 Qianwangang road, Qingdao, Shandong, China
[4]Institute of Chemistry and Chemical Technology, Mongolian Academy of Sciences, ave. Enkhtaivan, 54b, Ulaanbaatar, Mongolia

Article info

Received:
11 February 2022

Received in revised form:
5 March 2022

Accepted:
24 April 2022

Keywords:
Coal
Pyrolysis
Thermogravimetry
Plastometry
Activation energy

Abstract

The chemical composition, structural and plastometric properties of typical different-ranked coals from Mongolia deposits were studied. The non-isothermal iso-conversion Ozawa-Flynn-Wall method was used to assess kinetic parameters and to differentiate decomposition steps. Key peculiarities of the pyrolysis kinetics of brown and bituminous coals were revealed and discussed in terms of the composition and plastometric properties of coals. Brown coal was shown to undergo three decomposition steps with ever increasing activation energy as temperature increased because of the decomposition of thermally more and more stable molecular fragments. The pyrolysis of bituminous coals occurred in four steps, the activation energy having an extreme mode of temperature dependence. An important new finding was that the temperature range of the second, major pyrolysis step well corresponded to that between the softening and resolidification temperatures according to Gieseler plastometry, so that the decomposition of bituminous coals at the second step proceeded in a fluid-like medium, moreover, with constant activation energy. The yield and composition of the pyrolysis products obtained under isothermal conditions were also characterized depending on coal rank and temperature, and the ways for qualified utilizations were offered.

1. Introduction

Coal continues to be one of the main sources of energy worldwide and it is indispensable in the steel-making industry. Mongolia has large reserves of coals of various grades [1]. Currently, mainly brown and sub-bituminous coals are utilized for heat and electricity generation. However, direct combustion results in environmental problems. Also, coking coal is currently mined at the largest Tavantolgoi deposit to export to China for the production of metallurgical coke.

Much attention is paid in Mongolia to the development of coal processing into environmentally friendly energy carriers and valuable chemical substances and carbon materials. The results of the studies of the properties of some low-rank coals in the processes of thermal and thermochemical conversion [2–5], gasification [3, 6], and production of porous carbon materials [7] have been published in the literature. The coking properties of Tavantolgoi coal have been reported in [8, 9]. However, in general, the chemical composition and structure of Mongolian coals are still poorly investigated.

Coal pyrolysis is a fundamentally important process since it involves a set of chemical reactions, which play key roles in most coal conversion processes, such as coking, liquefaction, hydrogenation, gasification and combustion. Pyrolysis can be considered also a test reaction for coals because

*Corresponding author.
E-mail addresses: E-mail: kpn@akadem.ru

of the high sensitivity to coal properties. For all these reasons coal pyrolysis has been and is being studied from different perspectives [10–13]. Detailed information on pyrolysis kinetics is an actual objective to better understand decomposition phenomena, forecast chemical and physical changes and optimize conversion into valuable products [12, 14, 15]. Thermogravimetric analysis (TGA) in both iso-thermal and non-isothermal modes is the most common technique for studying the thermal properties and kinetics of coal pyrolysis [14, 16–20]. Based on the TGA measurements, some kinetic pyrolysis methods have been developed including model-fitting methods such as Freeman-Carroll [21], Coats-Redfern models [22] and model-free methods such as Friedman [23], Kissinger-Akahira-Sunose [24], Ozawa-Flynn-Wall [25–27]. Systematic trends in the kinetic parameters with coal rank and maceral composition have been found [18, 28–31]. The pyrolysis was shown to involve the rupture of different kinds of chemical bonds, the reactions with lower bond energies occurring generally at relatively low temperatures, while those with high energies at higher temperatures.

Of the coals of different ranks, bituminous coals of medium rank have specific physical properties: at a certain temperature, they can undergo a plastic state and then form strong coke at elevated temperature. Due to this valuable property, these coals are widely used in large-scale coke-making industry. However, few papers were devoted to the investigation of the pyrolysis kinetics of these coals [32, 33]. The authors [34] studied the pyrolysis kinetics of a series of bituminous coals, and also of non-bituminous coals for comparison. The pyrolysis of all the coals was reported to consist of three stages. The kinetic parameters for the main (second) decomposition stage estimated by the integral method obeyed general dependencies on the coal properties, such as rank, and indexes of chemical structure. The authors [33] also investigated the pyrolysis of different-ranked coals using distributed activation energy model. The activation energy values for the low-ranked coals were reported to increase gradually as coal conversion increased. However, bituminous coal of medium rank showed an extremal varying trend of activation energy versus conversion: the initial pyrolysis stage proceeded with an ever decreasing activation energy (from 313 to 240 kJ/mol), and then, when the pyrolysis conversion reached 40–50%, the activation energy commenced to increase gradually as conversion further increased. Such a specific pyrolysis behavior of bituminous coal was difficult to interpret reasonably based on the presented data of chemical and molecular compositions. Perhaps, this interesting phenomenon could result from the thermoplastic properties of coal, however, the relevant data were not presented.

The purpose of this paper was to study the chemical composition and structural properties of the typical coking and non-coking Mongolian coals, evaluate pyrolysis kinetics and find relations with the structural characteristics and thermoplastic properties. The kinetic parameters were estimated using the most developed Ozawa–Flynn–Wall (OFW) model-free method which allows the activation energy at various pyrolysis stages to be estimated. Also, the yield and composition of the isothermal pyrolysis products were characterized depending on the temperature and coal type.

2. Experimental

2.1. Coal samples and their chemical and structural characterization

2.1.1. Sample preparation and analytical characterization

The vitrinite-type coals from the Baganuur (B), Nariin Sukhait (N), and Tavantolgoi (T) deposits in Mongolia were used in this paper. The coals were ground (particle size of < 0.2 mm) and dried in a vacuum oven. The contents of moisture, ash, volatile matter and vitrinite reflectance were determined using standard procedures. The fluidity characteristics (softening point and re-solidification temperature) were determined using Gieseler plastometer, and plastic layer thickness by Sapozhnikov method. Ultimate analysis was performed using a Flash EATM 1112 analyzer. The content of metals in the ash was analyzed by the X-ray fluorescence method.

2.2. Structural characterization

The IRFT spectra were studied using KBr pellets prepared by a conventional technique [35, 36]. The spectra were recorded on a Nicolet 20-PC and Bruker Tensor-27 spectrometer within the wavenumbers of 400–4000 cm^{-1}. Multipoint correction of a baseline was conducted by built-in software. Based on the IRFT spectra, the semiquantitative index-es for aromaticity of hydrogen (H_{ar}) and carbon (C_{ar}) and CH_3/CH_2 ratio were estimated.

The X-ray diffraction patterns for the powdered coal samples packed into an aluminum holder were recorded using a PANalyticalX'Pert PRO diffractometer with Cu Kα radiation and step scanning (2θ = 0.2°, 25 s/step) between 2θ from 5° to 55°. The parameters of the stacking structure of the organic matter were determined from the (002) and (10) reflections corrected with absorption, polarization, and atomic scattering factors according to recommendations by [37].

2.3. Nonisothermal thermogravimetric and kinetic analysis

Thermogravimetric analysis (TGA) was carried out in a corundum crucible using a STA 449 F1 Jupiter instrument (NETZSCH) in the temperature range from 30 to 1000 °C in an argon flow (flow rates of shielding and purge gases were 20 and 50 mL/min, respectively). The results of the measurements were processed using the NETZSCH Proteus Thermal Analysis 5.1.0 software package supplied with the instrument. The kinetic characteristics were determined based on the TGA data obtained at the heating rates of 5, 10 and 20 deg/min. The kinetic parameters were estimated using Ozawa-Flynn-Wall (OFW) isocon-versional model-free method which has been successfully used previously [16] to study the kinetics of thermal decomposition of lignin.

2.4. Isothermal pyrolysis of coals

The isothermal pyrolysis tests were also carried out using a laboratory quartz retort to characterize the yield and composition of the products. After purging with nitrogen, the retort with coal was heated to a predetermined temperature and held for 80 min. The yields of the solid residue (char), tar and pyrogenic water were determined by weight, the yield of gases + losses by difference. Also, a bench scale unit with a tubular stainless steel reactor (volume of 1.5 L) was used to obtain larger amounts of products required for analytical measurements.

3. Results and discussion

3.1. The composition of coals

The samples used represented vitrinite-type coals (vitrinite content of more than 75%) with a few amount of ash. Shown in Tables 1 and 2 are the data on the proximate and ultimate analysis data. N and T coals showed coking ability, their plastic layer thicknesses were 10 and 16 mm, respectively. Brown coal exhibited no coking properties. The carbon and oxygen contents ranged 70.9 to 87.8% and 22.4 to 5.4%, respectively, following V^{daf} and $R_{o,r}$. All the coals showed low sulfur and nitrogen contents. These characteristics confirm the samples to correspond to brown coal (B) and two bituminous coals (N and T).

The composition of the ash from T coal was dominated by silicon (77.6 %) and aluminium compounds (15.7%); from N coal – by iron (27.5%), silicon (22.8%), aluminium (17.0%) and calcium (14.8%); from B coal – by calcium (40.4%), silicon (24.2%) and iron (17.4%).

Table 1
Proximate analysis of coal samples

Coal	A^d, wt.%	V^{daf}, wt.%	$R_{o,r}$, %	T_{soft},°C	T_{res}, °C	T, °C	y, mm
Baganuur, B	5.1	44.7	0.41	-	-	-	0
Nariin Sukhait, N	6.8	35.7	0.74	418	465	47	10
Tavantolgoi, T	8.2	27.7	1.12	429 [9]	499 [9]	70	16

$R_{o,r}$ – random vitrinite reflectance; T_{soft} – softening temperature; T_{res} – re-solidification temperature; ΔT – plasticity range; y – plastic layer thickness.

Table 2
Ultimate analysis data

Coal	wt.% on daf					H/C_{at}
	C	H	N	S	O	
Baganuur	70.9	5.2	1.0	0.5	22.4	0.88
Nariin Sukhait	84.4	4.8	1.6	1.0	8.3	0.68
Tavantolgoi	87.8	5.2	1.2	0.4	5.4	0.71

3.2. Structural characterization of coals

3.2.1. Characterization of molecular structure by IRFT spectra

The IRFT spectra showed strong absorbance at 3000–2750 cm^{-1} (stretching vibration of the aliphatic C-H bonds), at 1460–1440 cm^{-1} (bending vibration of CH_2 groups) and at 1376 cm^{-1} (bending vibration of CH_3) indicating the presence of a large amount of the aliphatic fragments. The absorbance at 1600 cm^{-1} (stretching vibration of the aromatic rings), at 3050 cm^{-1} (stretching vibration of the aromatic C-H bonds) and at 900–700 cm^{-1} (out-of-plane bending of the aromatic C-H bonds) reflect the presence of the aromatic fragments. The absorbances centered at 3400 cm^{-1}, 1750–1700 cm^{-1} and 1300–1000 cm^{-1} were attributed to various oxygenated fragments (phenolic hydroxyls, carbonyls, carboxyls, ester and ether groups, and alcohols). Brown coal featured an enhanced amount of oxygen-containing groups.

The characteristic absorbance at the 3100–2750 cm^{-1} spectral region was subjected to deconvolution into sub-bands related to aromatic (3100–3000 cm^{-1}) and aliphatic (3000–2750 cm^{-1}) C-H bonds. The assignments of the sub-bands were made following [35, 36, 38]. Based on the deconvoluted spectra (Fig. 1), the semi-quantitative aromaticity indexes for hydrogen (H_{ar}) and carbon (C_{ar}), and CH_3/CH_2 ratios were estimated.

In assessing the indexes we took account of the statistical data for bituminous coals that the ratio of the extinction coefficient for the stretching vibrations of the aliphatic C–H bonds to the extinction coefficient for the aromatic C–H bonds is 0.20; while the ratio for the extinction coefficient for the stretching vibrations of the CH_2 groups and CH_3 groups is 0.5. The indexes were calculated using the following formulas:

$$H_{ar} = \frac{A_{ar} / 0.2A_{al}}{1 + \left(\frac{A_{ar}}{0.2A_{al}} \right)} \quad (1)$$

$$\frac{CH_3}{CH_2} = 0.5 \times \left(\frac{A_{2955}}{A_{2923}} \right) \quad (2)$$

Carbon aromaticity Car index was estimated according to [39] based on the IRFT values for H_{ar} and the elemental analysis data.

Shown in Table 3 are the molecular indexes thus estimated. The values for H_{ar} and Car indexes decrease in the following order: Tavantolgoi – Nariin Sukhait – Baganuur following C^{daf}, V^{daf} and $R_{o,r}$. The CH_3/CH_2 ratios of 0.20 to 0.29 reflect different lengths of the aliphatic chains in the coals.

Table 3
Molecular indexes of organic matter of coals based on the IRFT spectra

Coal	Aromaticity index		CH_3/CH_2
	C_{ar}	H_{ar}	
B	0.66	0.19	0.29
N	0.76	0.36	0.20
T	0.76	0.41	0.23

3.2.2. Characterization of the spatial coal structure

The XRD patterns for coals showed typical broad and asymmetrical reflection in the 2Θ region from 8° to 34° due to intermolecular ordering of carbon matter and a weak reflection centered at 2Θ of about 44° due to intramolecular ordering.

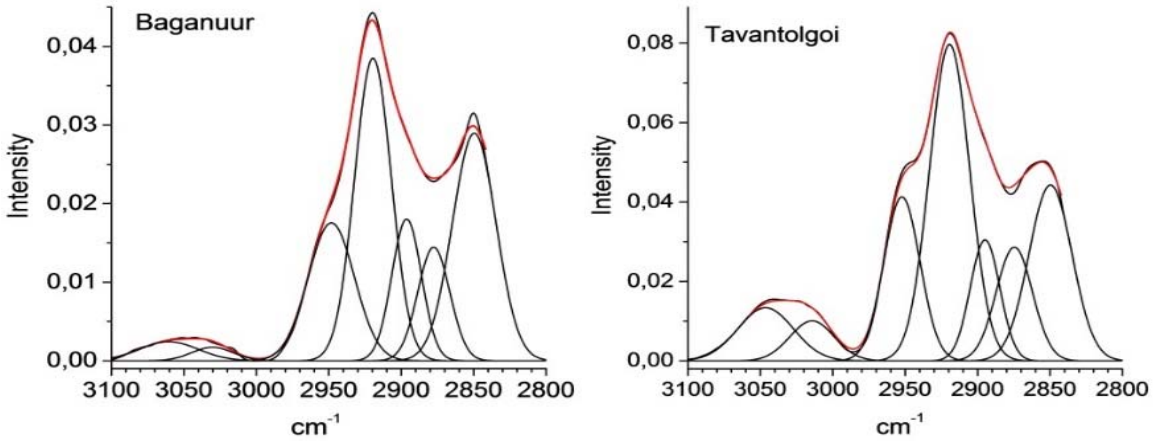

Fig. 1. The deconvoluted IRFT spectra for Baganuur and Tavantolgoi coals as examples.

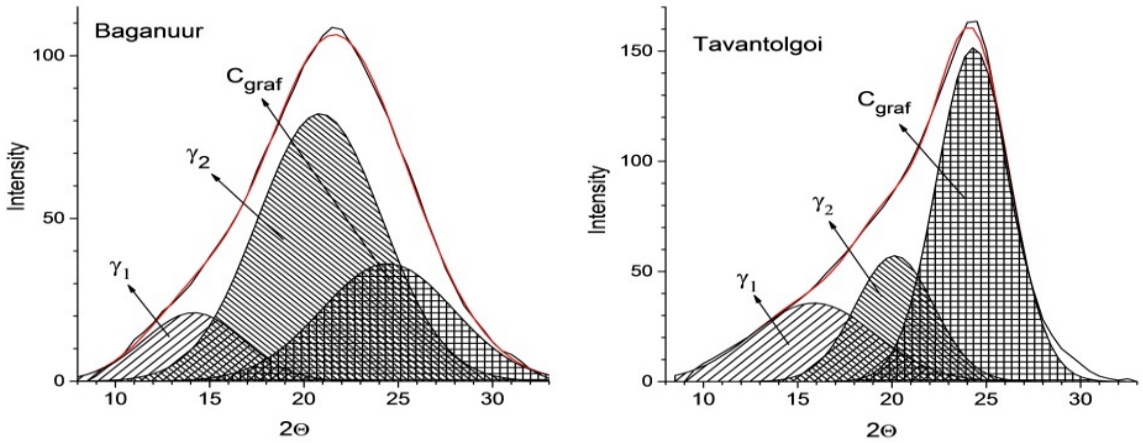

Fig. 2. The deconvoluted fragments of the XRD patterns for Baganuur and Tavantolgoi coals.

Table 4
The characterization of the spatial structure of coals

Coal	Proportion, %		Structural parameters of graphite-like component				A, %
	Graphite-like component	γ-component	d_{002}, Å	L_c, Å	L_a, Å	Number of layers, n	
B	31	69	3.64	9.62	22.9	3.6	45
N	49	51	3.62	13.2	24.0	4.6	64
T	57	43	3.66	17.3	20.7	5.7	75

Displayed in Fig. 2 are the fragments of the XRD patterns in the 2Θ range from 7 to 34° for two representative coals as examples. The curve-fitting analysis showed that the asymmetrical reflection attributed to the intermolecular ordering was best simulated by a superposition of three Gaussians which were assigned to a relatively ordered graphite-like component (C_{graf}) (at near 2Θ = 25°), to less ordered γ_1-component (2Θ of 19.0−19.5°) and to least ordered γ_2-component (2Θ of 10.0−10.5°). The graphite-like component is considered usually [40] as the stacks of the planar polycondensed aromatic clusters. Less ordered γ-components can involve mainly aliphatic fragments including naphthenes, alkanes and oxygen-containing groups spatially structured at the periphery of the graphite-like stacks.

The XRD data in Table 4 show the spatial structure of the organic coal matter to contain 31% to 57% of the fairly ordered graphite-like component. As the rank of coal increases, the number of layers (n) and the stack thickness (L_c) increase indicating the increase in the molecular ordering of the organic matter, the interlayer spacing (d_{002}) and layer diameter (L_a) remaining practically unchanged.

The proportion of the graphite-like component in the organic coal matter is generally considered to reflect coal aromaticity [40]. It can be drawn from the comparison of the C_{ar} values (in Table 3) and the proportion of the graphite-like component (in Table 4) that the latter in the brown coal contained only 45% of all the aromatic carbon atoms, and the remaining aromatic carbons occur in the amorphous γ-components (perhaps, in small and/or in highly substituted aromatic cycles) (Table 4). The polycondensed clusters in the bituminous N and T coals contain 64 and 75% of all the aromatic carbon atoms, respectively.

3.3. Non-isothermal pyrolysis of coals, TG/DTG results

Figure 3 shows the thermogravimetric (TG) and differential thermogravimetric (DTG) curves which reflect the temperature dependence of weight loss and the rate of weight loss, respectively.

The thermal stability indexes T_{init} (the temperature at the initial evolution of the volatile substances) and T_{max} (the temperature at a maximum rate of weight loss) were estimated based on the curve analyses. It can be seen from Table 5 that both T_{init} and T_{max} increase in order from B to N and to T coals, indicating that coals with more aromatic and more ordered structures are more stable,

hence, a higher temperature is required for decomposition. These results are consistent with the data reported in [18, 34].

3.3.1. The analysis of the pyrolysis kinetics

The dynamics of the pyrolytic decomposition of coals is considered generally [10] in terms of a stepwise process that involves a gradual desrupture of different chemical bonds which need corresponding activation energies for breaking. The isoconversional Ozawa-Flynn-Wall method was used to evaluate the kinetic parameters. The activation energy was determined from the following generalized expression for the rate of solid-phase reaction under non-isothermal conditions:

$$\frac{\mathrm{d}\alpha}{\mathrm{d}t} = \mathrm{kf}(\alpha) = \frac{A}{\beta}\exp^{\frac{-E}{RT}}\mathrm{f}(\alpha), \qquad (3)$$

where dα/dt is the rate of change of conversion (α) with time (t), A is the pre-exponential factor (min^{-1}), β is the heating rate (°C/min), E is the apparent activation energy (J/mol), R is the universal gas constant (8.314 J/mol·K), T is temperature (K), f(α) is the reaction model which is a function of conversion. Relative degree of coal conversion α can be defined as $\alpha = \frac{m_S - m}{m_S - m_f}$, where m_s and m_f are the initial and final weights of a sample, and m is its weight at a point of measurement. The integration of Eq. 3 after rearrangement yields the integral form of non-isothermal rate law given as follows,

$$\mathrm{g}(\alpha) = \int_0^{\alpha}\frac{\mathrm{d}\alpha}{\mathrm{f}(\alpha)} = \int_0^{T}\frac{A}{\beta}\exp\left(\frac{-E}{RT}\right)dT \qquad (4)$$

The fundamental expressions of kinetic methods to evaluate kinetic parameters from TGA data are based on the Eqs. 3 and 4.

Isoconversional methods are based on the principle that at a constant extent of conversion, the reaction rate is a function only of the temperature. Thus

$$\left[\frac{\mathrm{d}\ln\left(\frac{\mathrm{d}\alpha}{\mathrm{d}t}\right)}{\mathrm{d}T^{-1}}\right]_{\alpha} = -\frac{E}{R} \qquad (5)$$

It is a useful method for the estimation of activation energy despite the uncertainty of the reaction mechanism. It uses thermogravimetric data at multiple heating rates for the evaluation of activation energy as a function of conversion. The activation energy values obtained by isoconversional methods are termed as 'effective' or 'apparent' activation energy, to emphasize the presence of multistep kinetics where the activation energy tends to vary throughout the process.

Ozawa-Flynn-Wall method [25, 26] can be defined by the following equation:

$$\ln\beta = \ln\left[\frac{AE}{\mathrm{Rg}(\alpha)}\right] - 5.331 - 1.052\frac{E}{RT}, \qquad (6)$$

where g(α) is a constant at a given α conversion degree. By plotting ln(β) versus 1/T, the apparent activation energy E can be calculated based on slope.

The E values were calculated and plotted in Fig. 4 as a function of α, a degree of thermal decomposition of coal matter. It can be seen that the coals show quite different kinetic behavior. The initial decomposition of B coal proceeded with low activation energies (33–60 kJ/mol) that were close to that of 35 kJ/mol reported by [34] for the lignite decomposition at the first step. This can be due to cleavage of the weakest bonds, primarily oxygen-containing ones.

As the temperature increased, the decomposition of the organic matter of brown coal proceeded with ever higher activation energy; that is, the thermally more and more stable molecular fragments were involved in the decomposition reactions. Based on the profile of the curve for coal B, the pyrolysis process can be represented as consisting of three temperature stages that differed with activation energy. The second (middle) stage in a temperature range of 413–532 °C was characterized by fairly constant activation energy (near to 200 kJ/mol)) that may indicate the decomposition of similar types of chemical bonds.

Table 5
The thermal stability indexes of the coals derived from TG-DTG curves

Coal	Thermal stability index, °C		Coke yield, wt.% on daf
	T_{init}	T_{max}	
B	325	435	55.0
N	400	477	67.1
T	430	517	74.7

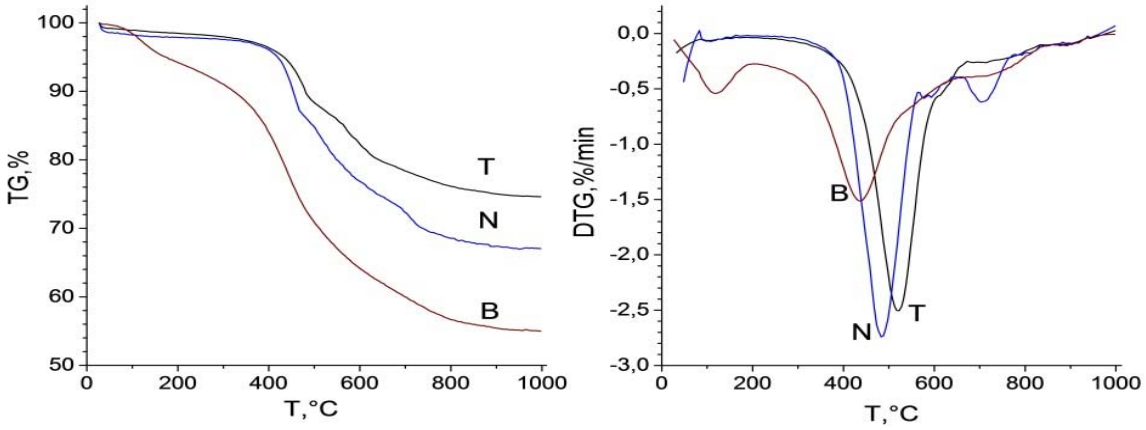

Fig. 3. TG/DTG curves of coal pyrolysis (heating rate of 10 °C/min).

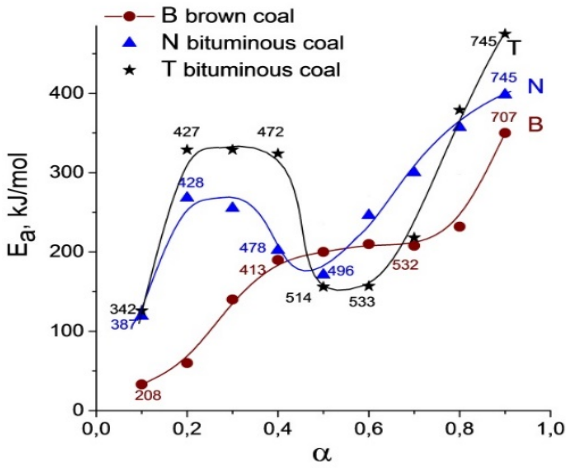

Fig. 4. The dependence of the activation energy (E_A) on the degree of conversion (α) of coals in the course of thermolysis (the figures at the curves are temperatures related to points).

The pyrolysis of the bituminous coals consisted of four steps distinguished by the activation energy. The first stage proceeded with higher activation energies compared to those for B coal. This could reflect the fact that they had less amount of weak C–O bonds and more amount of stronger aliphatic C–C bonds. As the temperature increased, increasingly ever stronger bonds were destructed. However, when the decomposition degree for the T coal has attained 0.2, the next pyrolysis step at the temperature range of 427–472 °C with fairly constant activation energy (about 330 kJ/mol) occurred. This step may indicate the radical reactions of a similar type which could involve the decomposition of bonds with an energy close to C–C in aliphatic linkages, including those between the aromatic units. However, when the decomposition degree for T coal attained 0.4 at 472 °C, the activation energy dropped greatly (to 150 kJ/mol) and then increased gradually as the temperature further increased. Both bituminous coals showed similar trends in the activation energy depending on conversion.

It should be noted that [33] also reported low-rank coals to show ever increasing activation energy as conversion increased. However, bituminous coal of medium rank showed an extremal trend, the first step proceeding with ever decreasing activation energy (from 313 to 240 kJ/mol.)

The specific pyrolysis kinetics for bituminous coals may be related to their ability to transition into a plastic state when heated due to the release of the initially present bitumen, as well as due to bitumen formed as a result of decomposition reactions. One can see from Table 1 that for both T and N coals an agreement is observed between the temperature range of the second pyrolysis step and that between the softening and resolidification points according to Gieseler plastometry. This indicated the fluid-like state of coals, N coal showing a narrower temperature range compared to T coal. So, this major step of thermal decomposition of the bituminous coals proceeded in a fluid-like medium practically with constant activation energy. The softening point and temperature range of plasticity are important indicators of the coking property of coals. One can conclude thus that the pyrolysis kinetics confirmed the higher coking ability of T coal compared to N coal.

Table 6

The molecular IRFT spectral indexes for pyrolysis tars

Coal	H_{ar} index	CH_3/CH_2
B	0.13	0.28
N	0.25	0.31
T	0.28	0.33

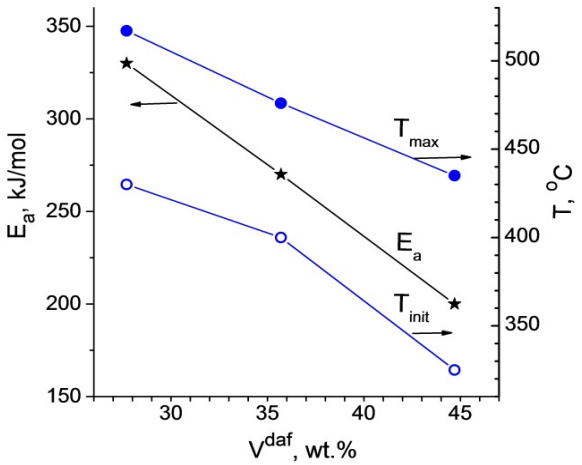

Fig. 5 The relations between the V_{daf} for coals and pyrolysis indexes T_{max}, T_{init} and E_a for the second pyrolysis stage.

At the third decomposition step for bituminous coals, the competing polycondensation reactions in the metaplast matter could dominate initiating nucleation followed by the generation of a solid char and its re-structuring yielding carbon oxides, methane, hydrogen and water. These reactions, which are predominantly exothermic [10], can proceed with reduced activation energy. The last stage of pyrolysis could be related to solid phase reactions of dehydrogenation, dealkylation and polycondensation with the increased activation energies, as in the case of the solid-phase decomposition of brown coal.

The data on the activation energies for the second main pyrolysis stage and on the T_{max} and T_{init} thermal stability indexes are plotted in Fig. 5 as functions of V^{daf} for coals.

It can be seen that the kinetic pyrolysis indexes for both brown and bituminous coals at the main second stage are in common, close to linear-, dependences on the V^{daf} yield. This result is consistent with the data reported by [34].

3.2. Isothermal coal pyrolysis tests

The isothermal pyrolysis tests were carried out to evaluate the yields and compositions of the products depending on the properties of coals and temperature. Figure 6 shows the yields of the coke residue, liquid tar and gases obtained from the pyrolysis of different coals at temperatures of 500, 600 and 700 °C. The yield of coke residue increased as coal rank increased. Brown coal yielded much more liquid tar at a lowered temperature of 500–600 °C (6–7%) compared to bituminous coals. The tar yields from the latter increased to 3.5–4.0 wt.% as the temperature increased to 700 °C.

The chars produced differed from the original coals with much less volatiles (6 to 16%) and with higher calorific values (6800 to 8200 kCal/kg). So, they can be used as a smoke-less and high-calorific solid fuel with lower emissions of greenhouse and harmful gases, as a metal reducing agent in pyrometallurgy and as a feedstock for the preparation of multi-purpose carbon materials.

The liquid tars were characterized by the IRFT spectra, group analyses and by fractionation distillation. The IRFT spectra showed strong absorbances at 3000–2750 cm^{-1}, 1460–1440 cm^{-1} and 1378 cm^{-1} which are characteristic of the aliphatic structures. The absorbances centered at 3025 cm^{-1}, 1600 cm^{-1} and 900–700 cm^{-1} indicated aromatic structures, the spectra for the brown coal tar showing smaller absorbance compared to tars from the bituminous coals. The profiles of the 900–700 cm^{-1} spectral region indicated the condensed structure of the aromatic rings in the molecules of tars from the bituminous coals. The presence of oxygen-containing compounds was indicated by the absorbances centered at 3400 cm^{-1}, 1620–1750 cm^{-1} and 1000–1200 cm^{-1}, the spectra for brown coal tar showing larger absorbances compared to other once. The semi-quantitative IRFT molecular indexes for tars are compared

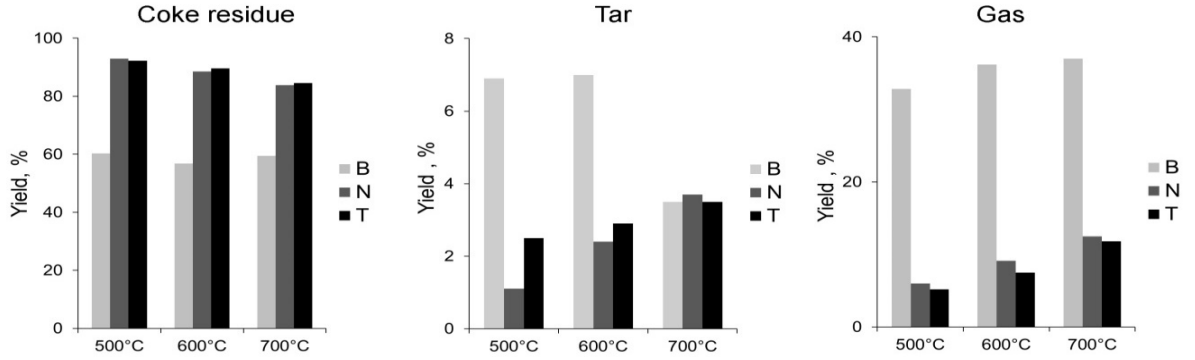

Fig. 6. The yields of products from the pyrolysis of coals at different temperatures.

Table 7
Group composition of pyrolysis tars

Coal	Group composition, wt %				
	Bases	Acids	Phenols	Asphaltenes	Neutral oils
B	3.0	2.0	14.2	19.2	61.6
N	11.	2.7	3.2	12.5	80.5
T	1.2	1.2	3.3	18.8	75.5

in Table 6. In general, the IRFT spectra showed the brown coal tar to be represented by a large number of aliphatic substances as well as by oxygen-containing groups; and the tars from the bituminous coals contained an increased amount of the polycondensed aromatic substances. The semi-quantitative H_{ar} aromaticity indexes for tar produced were less and the CH_3/CH_2 ratios were close to those for the parent coals.

The data on the group composition of coal tars are shown in Table 7. The predominant part was represented by the neutral oils, the largest oil yield (80.5%) being characteristic of tar from the N coal. Asphaltenes and phenols were present in fewer amounts, and the organic acids and bases accounted for no more than 2.5–5.0%.

According to distillation, the brown coal oil consisted of 82.6% of gasoline and kerosene fractions and 17.4% of non-volatile residue. The oil from the bituminous N coal contained much less distillate fraction (26.5%), and the main part (73.5%) accounted for non-volatile residue. The oil from the T coal differed with a high viscosity, only a little gasoline was distilled off, and non-volatile residue represented a pitch-like solid matter at ambient temperature.

The data on the product yields, group and fractional composition of the tars obtained from the pyrolysis of different coals make it possible to optimize the pyrolysis process to obtain the targeted products. The chars produced had a low content of the volatile matter and high calorific value. They can be used as a smokeless solid fuel of high calorific value (especially important for Mongolia), as a reducing agent in metallurgy, in iron- and steel-making and in ferroalloy production, in particular, as well as for the manufacturing of carbon materials for various needs. The distillate fractions of brown coal oil can serve as a feed-stock for valuable chemicals. Also, they can be catalytically hydrorefined to produce motor fuels. The pitch-like residue from the distillation of the neutral oils can be used as a binding agent.

4. Conclusions

The chemical composition, structural and plastometric properties of typically brown and bituminous coals from Mongolia deposits were characterized by different techniques. Their pyrolysis behaviors were studied using the non-isothermal and isothermal methods and the results were discussed in terms of the chemical, physical and plastometric properties.

Key stages of the pyrolysis of brown and bituminous coals were revealed based on the kinetic parameters determined using the iso-conversion Ozawa–Flynn–Wall method. The brown coal was shown to undergo three solid-phase decomposition steps, the first and third ones proceeding with ever higher activation energy as temperature increased because of the decomposition of thermally more and more stable molecular fragments.

The pyrolysis of the bituminous coals differed with more complicated kinetics, it occurred in four steps, the activation energy having an extreme mode of temperature dependence. An important new finding was that the temperature range of the second, major pyrolysis step well corresponded to that between the softening and resolidification temperatures according to Gieseler plastometry, so that the decomposition of bituminous coals at the second step proceeded in a fluid-like medium, moreover, with constant activation energy.

The yield and composition of the pyrolysis products obtained under isothermal conditions were also characterized depending on coal rank and temperature, and the ways for qualified utilizations were offered.

Acknowledgment

This work was funded by RFBR (Project No. 19-53-44001) and by the Fund for Science and Technology of Mongolia (Grant No. SHUGH/OHU/-2019/13) and also within the framework of the State Assignment (No. 0287-2021-0014)

for the Institute of Chemistry and Chemical Technology SB RAS using the instruments of the Krasnoyarsk Regional Research Equipment Centre of SB RAS.

References

[1]. B.-O. Erdenetsogt, I. Lee, D. Bat-Erdene, L. Jargal, *Int. J. Coal Geol.* 80 (2009) 87–104. DOI: 10.1016/j.coal.2009.08.002

[2]. A. Ariunaa, B. Zongqing, B. Jin, J. Narangerel, B. Purevsuren, F. Zhihao, H. Ranran, H. Chong, *Carbon Resour. Convers.* 4 (2021) 19–27. DOI: 10.1016/j.crcon.2021.01.005

[3]. B. Avid, B. Purevsuren, J. Temuujin, *Advances in Energy Research* 22 (2016) 159–178.

[4]. B. Purevsuren, Y. Davaajav, S. Batbilig, J. Namkhainorov, F. Karaca, T.J. Morgan, P.A. Rodriguez, F.H. Tay, S. Kazarian, A.A. Herod, R. Kandiyoti, *Adv. Chem. Engineer. Sci.* 3 (2013) 130–144. DOI: 10.4236/aces.2013.32016

[5]. B. Purevsuren, S. Batbileg, L.I. Kuznetsova, D. Batkhishig, G. Namkhainorov, P.N. Kuznetsov, *Solid Fuel Chem.* 53 (2019) 65–70. DOI: 10.3103/S0361521919020101

[6]. P.N. Kuznetsov, S.M. Kolesnikova, L.I. Kuznetsova, L.S. Tarasova, Z.R. Ismagilov, *Solid Fuel Chem.* 49 (2015) 80–86. DOI: 10.3103/S0361521915020068

[7]. U. Gombojav, I. Jambal, E. Byambajav, *J. Miner. Mater. Char. Eng.* 8 (2020) 97–106. DOI: 10.4236/jmmce.2020.83007

[8]. M.L. Ulanovsky, A.N. Likhenko, *Coke Chem.* 6 (2009) 13–20. DOI: 10.3103/S1068364X09060040

[9]. N.I. Fedorova, T.S. Manina, Z.R. Ismagilov, B. Avid, *Solid Fuel Chem.* 49 (2015) 129–134. DOI: 10.3103/S0361521915030064

[10]. P.R. Solomon, M.A. Serio, E.M. Suuberg, *Prog. Energy Combust.* 18(1992) 133–220. DOI: 10.1016/0360-1285(92)90021-R

[11]. J. Yan, Q. Yang, L. Zhang, Z. Lei, Z. Li, Z. Wang, S. Ren, S. Kang, H. Shui, *Carbon Resour. Convers.* 3 (2020) 173–181. DOI: 10.1016/j.crcon.2020.11.002

[12]. S. Niksa, *Energy Fuels* 5 (1991) 673–683. DOI: 10.1021/ef00029a008

[13]. R. Kandiyoti, A. Herod, K. Bartle, T. Morgan. Solid fuels and heavy hydrocarbon liquids. In: Thermal Characterization and Analysis (2nd ed.), 2016. DOI: 10.1016/B978-0-08-100784-6.00002-3

[14]. A. Arenillas, F. Rubiera, C. Pevida, J. Pis, *J. Anal. Appl. Pyrol.* 58–59 (2001) 685–701. DOI: 10.1016/S0165-2370(00)00183-2

[15]. G.N. Pretorius, J.R. Bunt, M. Gräbner, H. Neomagus, F.B. Waanders, R.C. Everson, C.A. Strydom, *J. Anal. Appl. Pyrol.* 128 (2017) 156–167. DOI: 10.1016/j.jaap.2017.10.014

[16]. O.Y. Fetisova, N.M. Mikova, O.P. Taran, *Kinet. Catal.* 61 (2020) 846–853. DOI: 10.1134/S0023158420050043

[17]. M. Kumar, A.M. Akhtar, V. Kumar, S. Liu, C.-Z. Li, H. Vuthaluru, *Chemical Engineering Journal Advances* 8 (2021) 100159. DOI: 10.1016/j.ceja.2021.100159

[18]. C. Geng, S. Li, C. Yue, Y. Ma, *J. Energy Inst.* 89 (2016) 725–730. DOI: 10.1016/j.joei.2015.04.004

[19]. S. Zhang, F. Zhu, C. Bai, L. Wen, C. Zou, *J. Anal. Appl. Pyrol.* 104 (2013) 660–666. DOI: 10.1016/j.jaap.2013.04.014

[20]. Y. Xu, Y. Zhang, G. Zhang, Y. Guo, J. Zhang, G. Li, *J. Therm. Anal. Calorim.* 122 (2015) 975–984. DOI: 10.1007/s10973-015-4801-z

[21]. N.A. Liu, W.C. Fan, *Thermochim. Acta* 338 (1999) 85–94. DOI: 10.1016/S0040-6031(99)00197-5

[22]. R. Ebrahimi-Kahrizsangi, M.H. Abbasi, T. *Nonferr. Metal. Soc.* 18 (2008) 217–221. DOI: 10.1016/S1003-6326(08)60039-4

[23]. H.L. Friedman, *J. Polym. Sci. Part C: Polym. Symp.* 6 (1964) 183–195. DOI: 10.1002/polc.5070060121

[24]. R.K. Mishra, K. Mohanty, *Bioresour. Technol.* 251 (2018) 63–74. DOI: 10.1016/j.biortech.2017.12.029

[25]. J.H. Flynn, L.A. Wall, *J. Polym. Sci. Part B: Polym. Lett.* 4 (1966) 323–328. DOI: 10.1002/POL.1966.110040504

[26]. T. Ozawa, *Bull. Chem. Soc. Jpn.* 38 (1965) 1881–1886. DOI: 10.1246/BCSJ.38.1881

[27]. W. Zheng, L. Liu, X.Y. Zhao, J.W. He, A. Wang, T.W. Chan, S. Wu, *Polym. Degrad. Stabil.* 120 (2015) 377–383. DOI: 10.1016/j.polymdegradstab.2015.07.024

[28]. C.-Z. Li, *Fuel* 112 (2013) 609–623. DOI: 10.1016/j.fuel.2013.01.031

[29]. Z. Gao, M. Zheng, D. Zhang, W. Zhang, *J. Energy Inst.* 89 (2016) 544–559. DOI: 10.1016/j.joei.2015.07.002

[30]. Z. Niu, G. Liu, H. Yin, C. Zhou, D. Wu, B. Yousaf, C. Wang, *Energ. Convers. Manage.* 124 (2016) 180–188. DOI: 10.1016/j.enconman.2016.07.019

[31]. H. Song, G. Liu, J. Zhang, J. Wu, *Fuel Process. Technol.* 156 (2017) 454–460. DOI: 10.1016/j.fuproc.2016.10.008

[32]. W. Du, G. Wang, Y. Wang, X. Liu, *Appl. Therm. Eng.* 152 (2019) 169–174. DOI: 10.1016/j.applthermaleng.2019.02.092

[33]. J. Yan, M. Liu, Z. Feng, Z. Bai, H. Shui, Z. Li, Z. Lei, Z. Wang, S. Ren, S. Kang, H. Yan, *Fuel* 261 (2020) 116359. DOI: 10.1016/j.fuel.2019.116359

[34]. M.D. Casal, M.F. Vega, E. Diaz-Faes, C. Barriocanal, *Int. J. Coal Geol.* 195 (2018) 415–422. DOI: 10.1016/j.coal.2018.06.014
[35]. M. Sobkowiak, P.C. Painter, *Fuel* 71(10) (1992) 1105–1125. DOI: 10.1016/0016-2361(92)90092-3
[36]. M. Sobkowiak, P.C. Painter, *Energy Fuels* 9 (1995) 359−363. DOI: 10.1021/EF00050A022
[37]. L. Lu, V. Sahajwalla, C. Kong, D. Harris, *Carbon* 39 (2001) 1821–1833. DOI: 10.1016/S0008-6223(00)00318-3
[38]. J. Alcañiz-Monge, D. Cazorla-Amoros, A. Linares-Solano, *Fuel* 80 (2001) 41−48. DOI: 10.1016/S0016-2361(00)00057-0
[39]. S. Supaluknari, F.P. Larkins, P. Redlich, W.R. Jackson, *Fuel Process. Technol.* 23 (1989) 47–61. DOI: 10.1016/0378-3820(89)90043-X
[40]. J.G. Speight, Handbook of coal analysis, 2th ed, Wiley, New Jersey, 2015. DOI: 10.1002/9781119037699